Intermolecular Vibrations of Phenol(H2O)2−5 and Phenol(D2O)2−5-*d*1 Studied by UV Double-Resonance Spectroscopy and ab Initio Theory

Ch. Jacoby, W. Roth, M. Schmitt, Ch. Janzen, D. Spangenberg, and K. Kleinermanns*

Institut für Physikalische Chemie und Elektrochemie I, Heinrich-Heine Universität Düsseldorf, Universitätsstrasse 1, D-40225 Düsseldorf, Germany

Received: January 5, 1998; In Final Form: March 18, 1998

The intermolecular vibrations of jet-cooled phenol(H2O)2−5 and phenol(D2O)2−5-d_1 were investigated in the S_0 and S_1 electronic states by using mass-selective UV spectral hole burning (SHB) and single vibronic level dispersed fluorescence (DF) spectroscopy. Phenol(H2O)2 shows broad bands with congested structure. We succeeded in obtaining its intermolecular vibrations via double-resonance spectroscopy. Previous studies of phenol(H2O)3 were completed. By employing soft two-color ionization and spectral hole burning, the vibronic spectra of phenol(H2O)4 and phenol(H2O)5 were unambiguously assigned according to cluster size and discriminated for possible isomers. An essentially complete picture of the vibronically active intermolecular vibrations was obtained. This was possible because SHB proves to be sensitive to the higher frequency intermolecular vibrations which tend to fast intramolecular S_1 vibrational relaxation in the larger clusters and therefore are of low intensity or absent in the two-color ionization spectra. The experimental results are compared to normal mode calculations based on fully optimized cluster structures obtained from ab initio studies at the Hartree−Fock level. Phenol(H2O)2−4 exhibit cyclic structures of the water moiety, while in case of phenol(H2O)5 the cyclic and a bridged "double-donor" structure are of comparable energy. The $6n - 6$ intermolecular vibrations of the cyclic clusters with $n \geq 3$ monomers can be classified into three small amplitude mutual rotations of the phenyl ring and the oxygen moiety, $2n - 6$ oxygen ring deformation vibrations, n intermolecular stretch vibrations, and $3n - 3$ hindered rotations of the water molecules in the cluster. The "double-donor" clusters exhibit a strong coupling of some of these modes. Many of the intermolecular vibrations, especially the mutual ring motions and the stretch vibrations, are optically active and can be assigned in the S_0 state by comparison with the calculated vibrational frequencies and deuteration shifts. The propensity rule helps to assign the corresponding vibrations in the S_1 state.

1. Introduction

Comprehension of the nature of hydrogen bonds is the key to a variety of phenomena in biology, chemistry, and physics. Among them, there are topics like solvation of molecules, folding of proteins, phase changes, the bulk properties, and surface structures of ice and liquid water.

The hydrogen-bonded clusters of phenol with water are of great interest because they are plain model systems for the investigation of hydrogen-bonded systems and solvent−solute interactions. Due to the aromatic chromophore, these clusters can easily be observed in supersonic molecular beams by standard spectroscopical methods such as laser-induced fluorescence (LIF), resonance-enhanced two-photon ionization (R2PI), and single vibronic level dispersed fluorescence (DF). Their size assignment is comparably straightforward when mass-resolved R2PI is used. The most important merit, however, is the ability of electronic spectroscopy to measure the important *inter*molecular vibrations of hydrogen-bonded clusters nearly completely.

Small clusters of phenol with water were first investigated by Lipert and Colson[1] by means of mass-selected multiphoton ionization. Stanley and Castleman performed two-color photoionization and cluster ion dip spectroscopy (CIDS) on phenol(H2O)0−4.[2] From their experiments they deduced that two

isomers of phenol(H2O)4 may exist with electronic origins at −180 and −50 cm⁻¹, respectively, relative to the phenol 0_0^0 transition.

Lipert and Colson showed by spectral hole burning (SHB) that the broad origin ($\approx$20 cm⁻¹) of phenol(H2O)2 is due to only one species in the electronic ground state.[3] A deconvolution of their spectra suggests that there may be a progression of very low frequency vibrations (3 or 6 cm⁻¹) in the S_1 electronic state. The minimum energy structure of phenol(H2O)2 in the ground state is cyclic, where every monomer acts both as proton donor and acceptor.[4,5] The calculated normal modes for this state have already been published[5] and are given in this paper for comparison only. The congestion of the S_1 spectrum may arise from a ring opening of the cyclic S_0 structure upon electronic excitation.[5]

The structure and vibrations of phenol(H2O)3 have been investigated in our group in the S_1 electronic state[6] and by Bürgi et al. in the ground and first excited states.[7] This cluster was described as a cyclic arrangement of the four monomers, with each of them acting both as proton donor and proton acceptor in analogy with the water tetramer.[7]

Watanabe et al. investigated the phenol(H2O)1−4,5(?) clusters by IR and Raman UV double-resonance spectroscopy in the region of the OH stretch vibrations.[8,9] They showed that the phenol(H2O)2−4 clusters have a cyclic arrangement of the hydrogen-bonded monomers because the frequency gap between

---

* To whom correspondence should be addressed.

the "bonded" and "free" stretch vibrations of the water molecules increases with increasing cluster size, in agreement with theory.[8,9] Upon analysis at the position of Stanley and Castleman's proposed second isomer of phenol(H$_2$O)$_4$ (36 302 cm^{-1}) they observed a spectrum with a different IR band pattern. Four transitions were found in the region of the "frequency gap". From ab initio calculations[10] they deduced that the appearance of vibrational transitions in this frequency region is due to water molecules which act as proton "double donors". This can only be expected for noncyclic clusters geometries such as "book"- or "cage"-like structures (cf. Figure 3). No final assignment of the electronic transition at 36 302 cm^{-1} either to phenol-(H$_2$O)$_4$ or to phenol(H$_2$O)$_5$ is given in refs 9 and 10.

Until now, no intermolecular vibrations of phenol(H$_2$O)$_{4,5}$ have been reported for the ground or first excited states.

2. Experimental Section

The resonant two-photon ionization (R2PI) measurements were carried out using the frequency-doubled output of a Nd:YAG (Spectra Physics, GCR170) pumped dye laser (LAS, LDL205) operated with Fluorescein 27 (nearly 200 μJ pulse energy). For spectral hole burning another Nd:YAG (Spectra Physics GCR3) pumped dye laser (LAS, LDL205) with second-harmonic generation (SHG, nearly 800 μJ pulse energy) counterpropagates the first laser in the ionization region. The second harmonic of the hole-burning laser was used together with its fundamental to improve the hole-burning signal.

The apparatus used for spectral hole burning and for R2PI consists of a source chamber pumped with a 1000 L/s oil diffusion pump (Alcatel) in which the molecular beam is formed by expanding a mixture of helium, phenol, and water through the 300 μm orifice of a pulsed nozzle (General Valve, Iota One). The skimmed molecular beam (Beam Dynamics Skimmer, 1 mm orifice) crosses the laser beam(s) at right angles in the ionization chamber. The ions are extracted in a modified Wiley–McLaren type time-of-flight (TOF) spectrometer[11] perpendicular to the molecular and laser beams and enter the third (drift) chamber, where they are detected using multichannel plates (Galileo). Typical mass resolution of the spectrometer is $m/\Delta m = 500$. Ionization and drift chamber are pumped with a 150 L/s rotary pump (Leybold), respectively. The vacuum in the three chambers was 1×10^{-3} mbar (source), 5×10^{-5} mbar (ionization), and 1×10^{-7} mbar (drift region), respectively, with beam on. Ions produced by the intense hole-burning laser perturb the experiment in a 2-fold manner: they distort the electric acceleration field and saturate the MCP detector, thus decreasing the sensitivity for detection of the signal ions. For removal of the hole-burning ions, the voltage of the repeller plate is first set to a negative potential. Shortly before the analyzing laser crosses the molecular beam the field is reversed for 10 μs using a fast push–pull high-voltage switch (Behlke, GHTS60). For an optimal separation of hole burning and signal ions the lasers were delayed by 400–600 ns.

The resulting TOF signal was digitized by a 500 MHz oscilloscope (TDS 520A, Tektronix) and transferred to a computer, where the TOF spectrum was recorded by means of a program written in LabVIEW (National Instruments). This program allowed us to record as many mass traces as desired, control the scanning of the laser and display, and save and plot the spectrum.

The Q-switch of the laser(s), the TOF voltage ramp, and the HV switch were triggered by a digital delay generator (Stanford DG535) together with a home-built delay generator for the triggering of laser flash lamps and pulsed nozzle. Timing stability was better than 2 ns.

TABLE 1: Binding Energies for the Most Stable Cyclic Structure of Phenol(H$_2$O)$_4$ and Different Structures of Phenol(H$_2$O)$_5$. All Values Are Given in cm^{-1}

| | HF energy | corrections | | $D_e{}^b$ | ZPE^c | $D_0{}^d$ |
		MP2	BSSE^a			
ph(H$_2$O)$_4$						
(*Dudud*)	13 380	3675	−3671	13 384	−3427	9957
ph(H$_2$O)$_5$						
cyclic	16 339	4267	−4336	16 270	−4173	12 094
cage(1)	17 195	5244	−6096	16 342	−4678	11 664
cage(2)	16 691	5336	−6039	15 988	−4518	11 471
book(1)	16 908	5394	−5687	16 616	−4510	12 105
book(2)	16 407	5007	−5364	16 051	−4380	11 670

^{a} Calculated at the MP2/6-31G(d,p)//HF/6-31G(d,p) level of theory. ^{b} $D_e = E(\text{HF}) + \Delta(\text{MP2}) + \Delta(\text{BSSE})$. ^{c} Scaling factor = 1.0000. ^{d} $D_0 = D_e + \text{ZPE}$.

Dispersion of the single-level fluorescence was performed with a 1 m Czerny-Turner monochromator, equipped with a holographic grating with 2400 grooves/mm blazed to obtain UV spectra around 300 nm in second order and an intensified CCD camera with a resolution-limiting pixel size of 23 μm. A spectral resolution up to 1 cm^{-1} can be achieved. The resulting two-dimensional camera picture ($x =$ dispersion, $y =$ height of the entrance slit) is corrected for the y-curvature from the spherical aberration of the mirrors. A single dispersed fluorescence spectrum is obtained by summing the fluorescence of a few hundred laser pulses on the CCD chip and subtracting the background stray light (gas pulse off) from the same number of laser pulses. Fifty to 200 of these spectra are averaged to obtain spectra as shown in Figure 6 and Figure 8a,b. The pixel number−wavelength relation has to be calibrated carefully, e.g., with the scattered light from the jet at different excitation laser wavelengths.

The phenol−water clusters have been deuterated by coexpanding D$_2$O, kept at −5 °C, together with phenol-d_1 (Merck, p.a.) at room temperature in 1−2 bar of helium. Within a few hours the partially and completely deuterated clusters were in a sufficiently stable equilibrium, which allowed us to take spectra of the fully deuterated species. Deuteration of the aromatic ring could be excluded under these conditions via NMR spectroscopy.

3. Theoretical Results

The clusters of phenol with one,[12] two,[5] and three[7] water molecules have already been studied theoretically with respect to their intermolecular vibrations. The applied method (HF/6-31G(d,p)) has been found to estimate the harmonic intermolecular vibrational frequencies of the smaller phenol(water) clusters in quite good agreement with the experimental results.

3.1. Computational Details. Ab initio calculations at the Hartree−Fock level (6-31G(d,p) basis) were performed using GAUSSIAN 94.[13] All structures have been fully optimized. The SCF convergence criterion was 10^{-8} hartree, and the convergence criterion for the gradient optimization of the cluster structures was 15 $\times$ 10^{-6} hartree/bohr and hartree/deg, respectively.

The vibrational frequencies have been calculated at the optimized geometry via normal mode analysis using analytical gradients.

The stabilization energies D_e and D_0 in Table 1 were obtained as differences of the cluster and monomer energies and are corrected for the zero-point energy (ZPE) and the basis set superposition error (BSSE). Further details on the calculation of the stabilization energies are given in ref 14.

Intermolecular Vibrations of Phenol(H$_2$O)$_{2-5}$

J. Phys. Chem. A, Vol. 102, No. 24, 1998 **4473**

The GAUSSIAN logfiles of our calculations containing the optimized geometries and the normal mode analyses are available on our homepage.[15] They can be visualized using programs like GAUSSVIEW, MOLDEN, or XMOL.[16]

3.2. Relative Stability of Phenol(water)$_{4,5}$. The relative stability of different cluster geometries of phenol(H$_2$O)$_{4,5}$ is discussed in ref 14. Only a short summary of the results is given here.

For phenol(H$_2$O)$_4$ the most stable structure is a cyclic arrangement with phenol down and the free hydrogen atoms up, down, up, and down (*Dudud* configuration; cf. Figure 2). Three other conformers of this structure are calculated to be only 114 to 152 cm^{-1} less stable.[14]

Difficulties arise for the case of phenol(H$_2$O)$_5$. All ab initio calculations—corrected for the harmonic ZPE—show that the analogous cyclic water hexamer is the most stable configuration. However, from diffusion Monte Carlo simulations[17,18] taking account of anharmonic ZPE and from far infrared spectroscopy[19] a cage-like structure is expected to be at least predominant. Our ab initio calculations show that the cyclic arrangement of phenol-(H$_2$O)$_5$ (cf. Figure 3) is more stable than the "cage" structure if MP2 and zero-point energy contributions are included and if the energies are corrected for BSSE. Among the 10 structures we calculated, there is a "book" structure (cf. Figure 3) which has nearly the same energy as the cyclic cluster. We believe that the interaction of a free hydrogen atom with the aromatic π electrons is responsible for the higher stabilization energy; cf. the dashed line in Figure 3.

The most stable cage geometry cage(1) is less stable by 441 cm^{-1} than the book(1) structure if all corrections are included; cf. Table 1.

3.3. Intermolecular Vibrations. For hydrogen-bonded clusters, $6n - 6$ intermolecular vibrations for n monomers ($n - 1$ water molecules, 1 phenol molecule) can be expected which arise from conversion of three rotational and three translational degrees of freedom of every bound monomer. In the case of phenol with one,[12] two,[5] and three[7] water units, these normal modes have been described and assigned in the literature.

All intermolecular vibrations of the phenol(H$_2$O)$_{2-5}$ clusters are comprised of translational and rotational motions of the monomers against each other. The character of the original monomer displacement is preserved in most cases upon cluster formation. The intermolecular vibrations of the *cyclic* structures of phenol(H$_2$O)$_{2-5}$ can be divided into characteristic groups. The following types of displacements can be distinguished (in order of increasing energy) by the residual motion of the water units.

$3n - 3$ vibrations with translational parentage of the water monomers:

(i) three mutual ring motions

(ii) $2n - 6$ oxygen ring deformation vibrations

(iii) n hydrogen bond stretch vibrations

$3n - 3$ vibrations with rotational parentage of the water monomers:

(i) $n - 1$ torsions of the free, i.e., unbound, hydrogen atoms of the water molecules

(ii) $n - 1$ rotations of the hydrogen bound H atoms about the c-axis of the water molecules

(iii) $n - 1$ rotations of the hydrogen bound H atoms about the a-axis of the water molecules

The double donor (cage and book) clusters exhibit similar vibrations; cf. Table 2. It must be pointed out that coupling of these motions may occur if the vibrational energies are very similar. Therefore, a final assignment cannot be given in some

TABLE 2: Harmonic Frequencies and Approximate Description of the Intermolecular Vibrations for Phenol(H$_2$O)$_{2-5}$ As Obtained from the Normal Mode Analysis (HF/6-31G(d,p), Unscaled Values are Given in cm^{-1}

description	ph(H$_2$O)$_2$	ph(H$_2$O)$_3$	ph(H$_2$O)$_4$	ph(H$_2$O)$_5$ cyclic	cage(1)	book(1)
Mutual Motions of the Phenyl Ring and the Water Moiety						
butterfly	21.6	21.3	12.8	12.1	10.1	13.9
twist	41.2	29.6	25.8	20.3	28.8	27.8
cogwheel	63.0	45.7	33.3	27.0	32.7	47.3
Deformation Vibrations of the Water Moiety						
		69.3	41.3	34.5	50.0	38.9
		74.6	53.6	39.7	55.2	61.0
			64.7	46.2	64.7	70.7
			79.0	55.1	94.8	80.5
				73.6		91.8
				81.5		
Hydrogen Bond Stretch Vibrations						
	125.2[a]	153.2[a]	147.4[a,b]	135.0[a,b]	129.8[c]	143.0[c]
	170.2[b]	190.7[b]	187.5[a,b,d]	176.4[a]	146.3[a]	167.0[a]
	206.6	217.1	203.5[b]	183.8[b]	155.5[c]	175.6[a]
		237.6	241.6	232.5	183.5	186.5
			271.2	259.6	203.5	206.5[b]
				288.0	207.1[b]	218.2[d]
					233.9[d]	265.5
					230.7[d]	
Free Hydrogen Torsion (Water b-Axis Rotation)						
	189.1	195.9	182.9	168.7	242.0	215.5[e]
	269.5	233.4	216.5	194.8	254.4[e]	234.1
		296.4	253.1	223.9	292.9	247.5
			296.9	253.9		294.0
				287.0		
Bound Hydrogen Torsion (Water c-Axis Rotation)						
	301.5	327.0	355.0	338.6	366.3	329.4
	388.6	404.7	405.5	390.2	398.7	393.8
		433.3	421.3	409.8	428.7	410.9
			441.1	416.1	438.2	446.8
				446.2	520.3	507.0
					529.8	
Bound Hydrogen Torsion (Water a-Axis Rotation)						
	517.5	643.4	614.4	674.4	603.5	565.8
	676.6	750.0	751.9	744.5	636.1	637.3
		806.8[f]	801.4	760.4	669.2	703.8
		928.6[f]	848.4[f]	815.9[f]	782.7	757.9
		948.3[f]	931.3[f]	848.0[f]	804.3	818.7
			949.9[f]	913.5[f]	907.2	855.7[f]
						857.9[f]
						986.9[f]

[a] Phenol acceptor—water donor stretch vibration. [b] Phenol donor—water acceptor stretch vibration. [c] Double-donor water—hydrogen bond stretch vibration. [d] With contributions from free hydrogen torsional motion. [e] With contributions from hydrogen bond stretching motion. [f] With contributions from intramolecular phenol motions.

cases. Coupling with intramolecular vibrations of phenol can also be found; cf. Table 2. A comparison of the intermolecular vibrations of the phenol(H$_2$O)$_{2-8}$ with the corresponding pure water clusters (H$_2$O)$_{3-9}$ will be discussed in ref 14.

3.4. Mutual Ring Motions. From the ab initio calculations it turns out that the three low-frequency normal modes of the phenol(H$_2$O)$_{2-5}$ clusters can be described as hindered rotations of the aromatic ring and the hydrogen-bonded water moiety. These normal modes are indicated as ν_1, ν_2, and ν_3 and shown in Figure 1 for phenol(H$_2$O)$_3$ together with their respective rotational axis.

The lowest frequency motion always contains a rotation of phenol about its b-axis (cf. Figure 1). The whole normal mode can best be described as "butterfly" type motion ν_1 of the two moieties (phenyl ring and hydrogen-bonded network).[7] The calculated frequency decreases for the cyclic structures from 22 (phenol(H$_2$O)$_2$) to 12 cm^{-1} (phenol(H$_2$O)$_5$). For the book
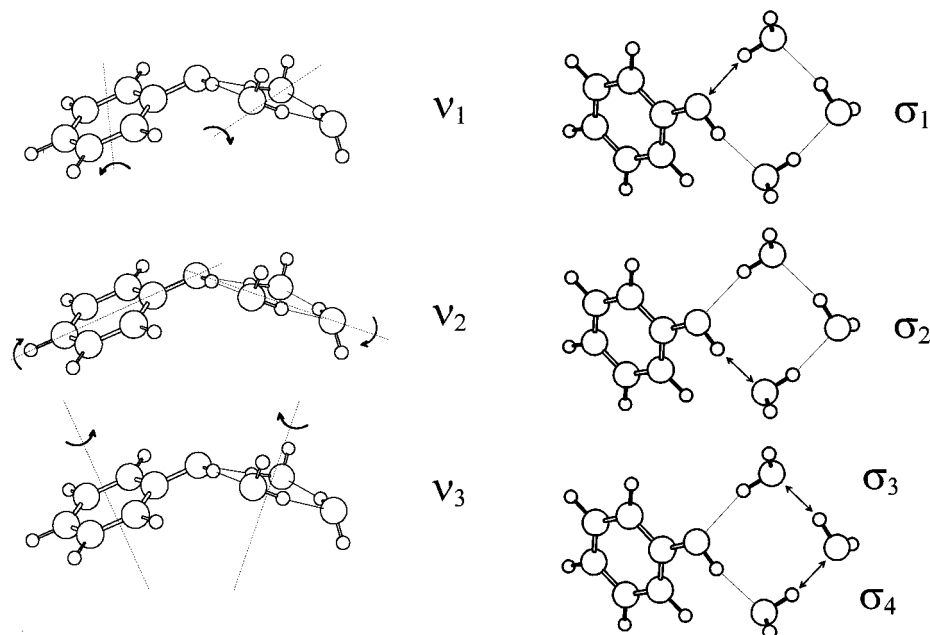
Figure 1. Schematic pictures of selected intermolecular vibrations of phenol$(H_2O)_3$. The three mutual ring motions ν_1, ν_2, and ν_3 and the corresponding rotational axes are displayed on the left side. On the right-hand side the four (isolated) hydrogen bond stretching vibrations $\sigma_1-\sigma_4$ are indicated by arrows: σ_1 is the phenol acceptor–water donor mode, σ_2 is the phenol donor–water acceptor mode, and σ_3 and σ_4 are the denoted displacements of the two water molecules.
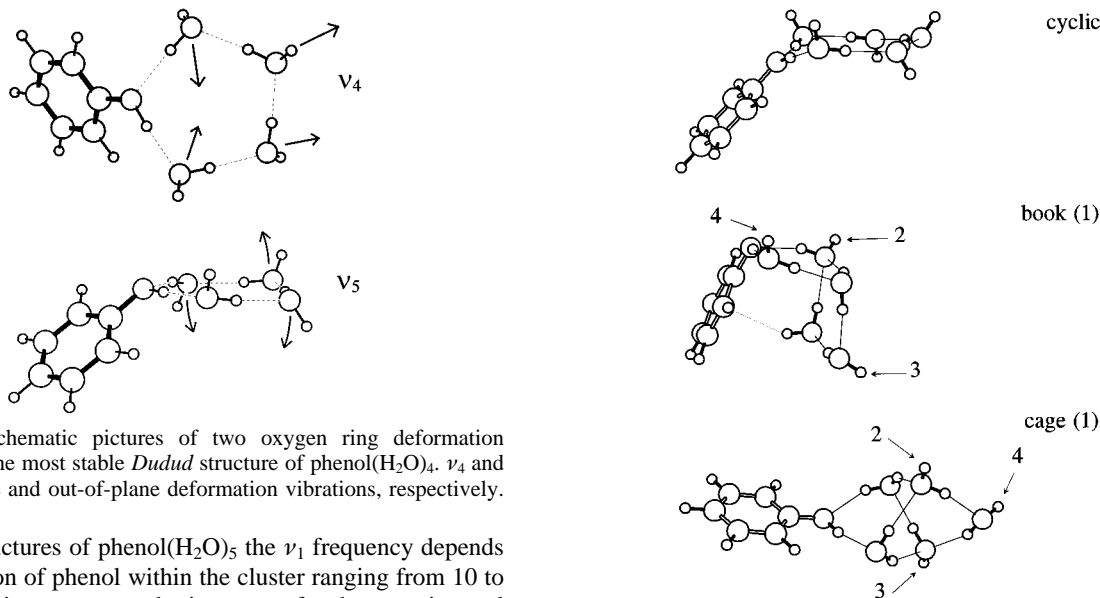
Figure 2. Schematic pictures of two oxygen ring deformation vibrations of the most stable *Dudud* structure of phenol$(H_2O)_4$. ν_4 and ν_5 are in-plane and out-of-plane deformation vibrations, respectively.

and cage structures of phenol$(H_2O)_5$ the ν_1 frequency depends on the position of phenol within the cluster ranging from 10 to 21 cm^{-1}. This turns out to be important for the experimental structure assignment; see below.

The ν_2 vibration looks like a mutual "twisting" of the aromatic ring and the water moiety of the cluster (*a*-axis rotation of phenol; cf. Figure 1) and decreases from 41 to 20 cm^{-1} with increasing oxygen ring size; cf. Table 2.

The remaining normal mode ν_3 may be described as a "cogwheel"-like rotation of the two rings against each other (*c*-axis rotation of phenol; cf. Figure 1). Its harmonic frequency decreases from 63 to 27 cm^{-1} with increasing number of monomers; cf. Table 2.

3.5. Ring Deformations. The deformation vibrations (approximately 30−100 cm^{-1}) of the hydrogen-bonded moiety can be identified unambiguously only for the cyclic clusters. For phenol$(H_2O)_{2,3,4,5}$ there are 0, 2, 4, 6 of these normal modes. Two of them are shown in Figure 2 for phenol$(H_2O)_4$. In the case of the book and cage structures of phenol$(H_2O)_5$ some of these deformation modes cannot be found anymore. The

Figure 3. Three structures of phenol$(H_2O)_5$. The cyclic arrangement is displayed on the top. The book(1) structure turns out to be the most stable geometry at the HF/6-31G(d,p) level of theory due to an additional van der Waals bond (indicated by the dashed line). The most stable cage structure is presented below. Other isomers can be obtained by replacing the free hydrogen atoms in the indicated positions 2, 3, or 4 by the phenyl ring; cf. Table 1 and ref 14.

frequencies of these vibrations are shifted toward higher wavenumbers and their motion appears as predominantly hydrogen bond stretch vibrations. Due to the larger number of hydrogen bonds which exceeds the number of monomers in the double donor clusters, there must be a larger number of stretch modes. The hydrogen bond stretch vibrations are expected in the region from 120 to approximately 250 cm^{-1}, while the deformation modes have energies below 100 cm^{-1}.

3.6. Hydrogen Bond Stretch Vibrations. In most clusters the hydrogen bond stretch vibrations can clearly be identified: The lowest frequency mode σ_1 of the cyclic clusters can always

be assigned to the water donor−phenol acceptor stretch motion (125−153 cm⁻¹). In the case of the book and cage structures of phenol(H_2O)₅ the hydrogen bond(s) involving the double donor water molecule(s) has the lowest stretch frequency; cf. Table 2. The phenol donor−water acceptor hydrogen bond stretch frequency remains quite constant for the cyclic phenol(H_2O)₃₋₅ but is increased considerably in the double-donor structures from 184 to 207 cm⁻¹; cf. Table 2. This turns out to be important for the experimental structure assignment; see below.

The remaining stretch modes are located between water units. In phenol(H_2O)₃, these vibrations are fixed on single hydrogen bonds (cf. Figure 1, σ_3 and σ_4). The water−water stretch modes are coupled to the phenol−water stretch vibrations in the larger clusters. Mutual coupling is observed as well.

In phenol(H_2O)₄, the stretch vibrations at 147.4 and 187.5 cm⁻¹ are symmetric and antisymmetric combinations of the phenol donor−water acceptor and the phenol acceptor−water donor stretch modes. Alternatively, the 147.4 cm⁻¹ vibration can be described as an oxygen ring breathing mode as well. The 135.0 cm⁻¹ mode of the cyclic form of phenol(H_2O)₅ is a very similar motion.

The vibrations at 129.8 and 155.5 cm⁻¹ of the cage form of phenol(H_2O)₅ are the symmetric and antisymmetric combinations of the two double-donor stretch vibrations. The modes at 167.0/175.6 and 186.5/265.5 are symmetric/antisymmetric combinations of the sidewall stretch modes of the book form. The mode at 167.0 cm⁻¹ is located at the side where phenyl is attached and can be regarded as a phenol acceptor−water donor vibration, too; cf. Table 2.
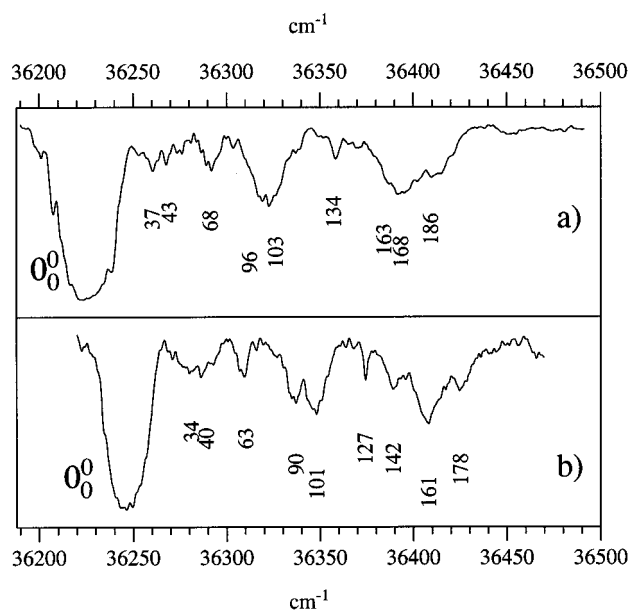
3.7. Intermolecular Vibrations of Rotational Origin. The torsion or flipping motion of the nonbound hydrogen atoms of the water molecules originates from the *b*-axis rotation of the single water units. They all appear in the frequency region between 190 and 300 cm⁻¹, i.e. partially in the region of the hydrogen bond stretch modes. The *b*-axis rotational origin can still be seen in the case of phenol(H_2O)₂. For the larger clusters the motions appear as torsional "flipping" of the unbound hydrogen atoms which can interconvert between the possible cluster conformers. In the case of the cyclic phenol(H_2O)₄ and the double-donor structures of phenol(H_2O)₅ some of the free hydrogen torsions couple to hydrogen bond stretch motions; cf. Table 2.

The next, in general very isolated, type of intermolecular vibrations are rotations of the bound hydrogen atoms (*c*-axis rotation of the water molecules) and can be found in the 300−530 cm⁻¹ frequency region. This description is more general than the ρ_2 nomenclature of phenol(H_2O)₁ or "out-of-plane libration" for phenol(H_2O)₃[7] because it can be applied to the double-donor structures as well.

The remaining intermolecular normal modes can be found between 480 and 990 cm⁻¹. They are motions of the bound hydrogen atoms arising from *a*-axis rotation of the water molecules. In most cases an unambiguous assignment is not possible here due to mixing of these normal modes with different intramolecular vibrations of phenol. Therefore more than $n - 1$ frequencies are given for these vibrations in Table 2.

4. Experimental Results and Discussion

4.1. SHB Spectra of Phenol(H_2O)₂. We succeeded in obtaining SHB spectra of the *inter*molecular vibrations of phenol(H_2O)₂ and phenol(D_2O)₂ as shown in Figure 4a,b. Similar to the electronic origin, the intermolecular vibrations of phenol(H_2O)₂ are broad (ca. 15 cm⁻¹). Table 3 shows a

Figure 4. Hole burning spectra of (a) phenol(H_2O)₂-*h* and (b) phenol-(D_2O)₂-*d₁* obtained by analyzing the electronic origin bands at approximately 36 226 and 36 248 cm⁻¹. Vibrational frequencies are given in cm⁻¹.

TABLE 3: Intermolecular Vibrational Frequencies of Phenol(H_2O)₂-*h* and Phenol(D_2O)₂-*d₁* in the S₁ State. For Assignment See Text (All Frequencies Are Given in cm⁻¹)

experimental S₁ frequencies		assign-ment	calculated harmonic S₀ frequencies[5]		alternate assignment
ph(H_2O)₂-*h*	ph(D_2O)₂-*d₁*		ph(H_2O)₂-*h*	ph(D_2O)₂-*d₁*	
0 (36 226)	0 (36 248)	0_0^0			$0_0^0/\nu_1$
37	34	ν_1	21.6	20.8	ν_2
43	40	ν_2	41.2	40.1	ν_3
68	63	ν_3	63.0	59.8	$2\nu_2$
96	90	σ_1	125.2	120.9	$3\nu_2$
103	101	$\nu_1+\nu_3$			σ_1
134	127	$2\nu_3$			$\sigma_1+\nu_2$
163	142	ν_4	189.1	133.6	ν_4
168	161	σ_2	170.2	163.5	σ_2
186	178	σ_3	206.6	198.3	σ_3

tentative correlation between the S₀ calculations of the harmonic frequencies of the cyclic cluster and the observed contours of the intermolecular vibronic S₁ state bands. The assignment is supported by the SHB spectra of phenol(D_2O)₂-*d₁*; that is, the assigned bands show the expected small deuteration shifts to lower frequencies.

The three lowest frequency vibrations ν_1, ν_2, and ν_3 are motions of the phenyl ring relative to the ring formed by the three oxygen atoms, as discussed in section 4.7. The other Franck−Condon active modes are the intermolecular stretch vibrations σ_1, σ_2, and σ_3, possibly the free hydrogen torsion ν_4, and several combination bands. As expected, the weak phenol acceptor−water donor H bond has a smaller force constant than the other H bonds and $\nu(\sigma_1) < \nu(\sigma_2,\sigma_3)$. Because of their large reduced masses and considerable force constants, the intermolecular stretch vibrations are supposed to be almost harmonic and therefore good approximations to experimental values. Deuteration shifts < 5% are predicted. The band at 163 cm⁻¹ is tentatively assigned to a free hydrogen torsion due to its considerable isotope shift; cf. Table 3.

The width of the bands cannot be explained by the calculated rigid cyclic minimum energy structure. No harmonic frequencies lower than 20 cm⁻¹ have been calculated. Measurements of the rotational constants of 1-naphthol(H_2O)₂ via rotational

coherence spectroscopy[22] point to a cyclic structure of this cluster, too. The R2PI spectrum shows narrow vibronic bands with no congestion from low-frequency bands.[23] Similar sharp bands should also be expected for phenol(H_2O)$_2$. In addition, the dispersed fluorescence spectrum of *p*-cresol(H_2O)$_2$ shows no resonance fluorescence but instead very broad fluorescence with a strong red shift.[20,24]

As proposed in ref 5, the following description of the spectroscopical and theoretical results can be given: The minimum energy structure of the electronic ground state is cyclic. A linear structure, derived from the opening of the weaker H bond of the "H donor" H_2O, is supposed to be another local minimum energy structure. In the S_1 state, transfer of electron density from the phenolic oxygen atom to the aromatic ring takes place and the O atom can be expected to be a worse H acceptor than in the S_0 state. Phenol(H_2O)$_2$ is less stable in the S_1 state than in the S_0 state, which leads to a comparably large vertical excitation energy. If we assume that in the S_1 state the linear structure is more stable than the cyclic arrangement, electronic excitation of the phenol(H_2O)$_2$ leads to a cyclic structure which couples strongly with vibrational modes of the linear structure. This coupling and the high vibrational mode density resulting from very low frequency vibrations of linear phenol(H_2O)$_2$ lead to a broadening of the electronic origin in the R2PI, SHB, and LIF spectra. Fluorescence transitions from the linear structure of the excited electronic state lead to a vibrationally excited linear structure of the electronic ground state, which is less stable than the cyclic structure. Hence the fluorescence is shifted to longer wavelengths relative to the excitation wavelength. Due to fast IVR in the S_1 state, no resonance fluorescence can be obtained. The broadening of the fluorescence can be explained by the high vibrational mode density of the linear structure in the S_0 and S_1 states.

4.2. R2PI, SHB, and DF Spectra of Phenol(H_2O)$_3$. The phenol cluster with three water molecules exhibit narrow ($\approx$2 cm^{-1}) vibronic bands in the R2PI and SHB spectra. Ab initio calculations[7] show a cyclic minimum energy *Udud* structure; cf. Figure 1. The RIDIR spectrum in refs 8 and 9 exhibits four low-frequency ("bound") OH stretch vibrations, in agreement with a cyclic structure. The SHB spectra of phenol(H_2O)$_3$ and phenol(D_2O)$_3$-d_1 displayed in Figure 5a,b show a 1:1 correspondence to the R2PI spectra; that is, only one isomer absorbs in this frequency range. Figure 6 displays dispersed fluorescence spectra of phenol(H_2O)$_3$ obtained by exciting the electronic origin and several intermolecular vibronic bands.

The assignment of the low-frequency fundamentals, ν_1, ν_2, and ν_3 and of the intermolecular stretch vibrations $\sigma_1-\sigma_4$ is given in Table 4. The bands at 9.6/16.9 cm^{-1} in the S_1/S_0 state can be assigned to the butterfly motion of the phenyl ring and the H-bonded ring analogously to phenol(H_2O)$_2$. Bürgi et al. observed a band at 11.3 cm^{-1} in their R2PI spectrum,[7] which we also observed in our R2PI and LIF spectra but not in the SHB spectrum; cf. Figure 5a. They assigned this band to the ν_1 vibration. We dispersed the fluorescence obtained from excitation of this band and found a DF spectrum with completely different frequencies than in the other phenol(H_2O)$_3$ DF spectra. Hence both the SHB and the DF spectra prove the band at 11.3 cm^{-1} to belong to another species. The band at 18.9 cm^{-1} is the first overtone of the ν_1 vibration, because its dispersed fluorescence spectrum shows a very strong propensity for a band at 33.2 cm^{-1} (2ν_1 in the S_0 state); cf. Figure 6b. The strong intensity of the 2ν_1 band and the existence of a ν_1 progression point to some change of the angle between the two rings upon S_1 excitation. The large Franck–Condon (FC) factor of the
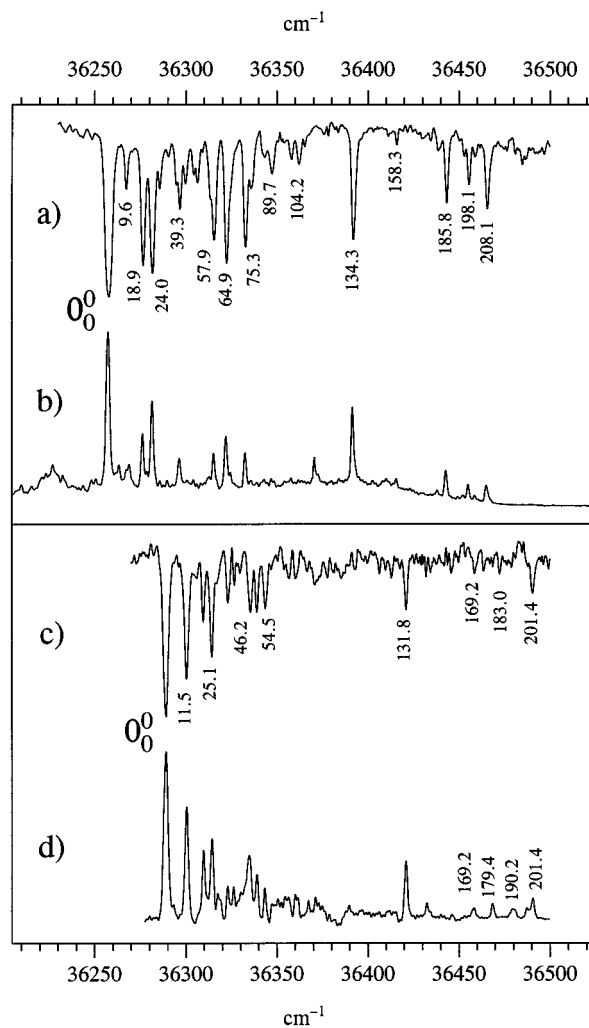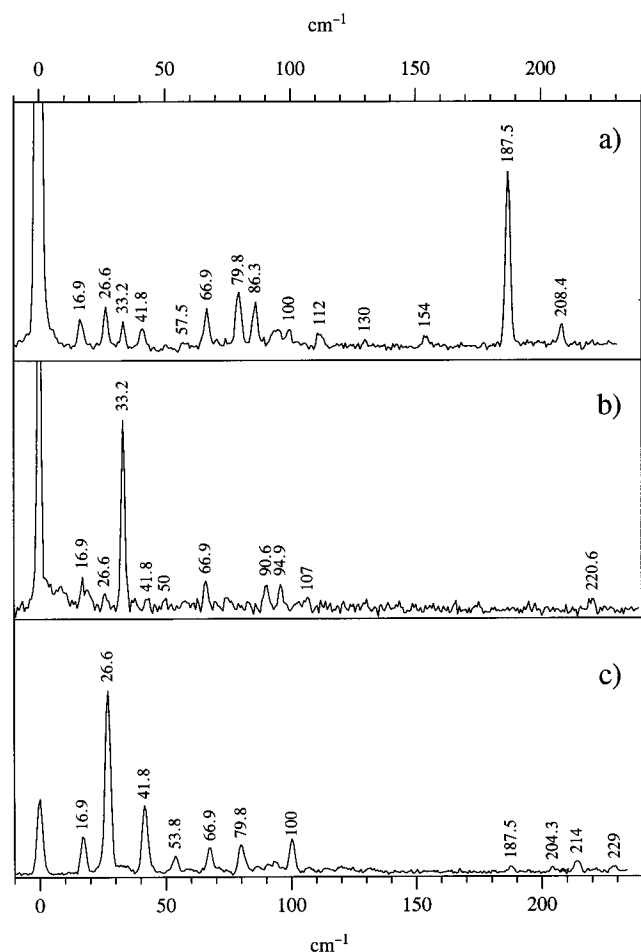

Figure 5. Hole burning and R2PI spectra of (a, b) phenol(H_2O)$_3$-*h* and (c, d) phenol(D_2O)$_3$-d_1 obtained upon analysis of the electronic origin bands at 36 257.8 and 36 289.4 cm^{-1}, respectively. Traces (a) and (c) show the SHB spectra. Vibrational frequencies are given in cm^{-1}.

2ν_1 vibration may arise from a Fermi resonance with the ν_2 motion. The next band at 24.0/25.1 cm^{-1} cannot be explained by overtone or combination bands and is assigned to the next fundamental ν_2, which is a mutual twisting of the two rings. The DF spectra in Figure 6a–c very nicely show the correlation 18.9/33.2 and 24.0/26.6 cm^{-1} according to the propensity rule. The phenol donor stretch vibration σ_2 is the most intense band when exciting the electronic origin similar as in phenol(H_2O)$_1$ and phenol(H_2O)$_4$.

Following the above procedure, we assign 3ν_1 (27.9/50.0 cm^{-1}), $\nu_1+\nu_2$ (32.5/– cm^{-1}), and finally ν_3 (39.3/41.8 cm^{-1}) for the S_1/S_0 state, respectively. The strong bands at 57.9/66.9 and 64.9/79.8 cm^{-1} are probably the two oxygen ring deformation bands ν_4 and ν_5 calculated at 69.3 and 74.6 cm^{-1}. An alternate assignment is 57.9 cm^{-1} as 2$\nu_1+\nu_3$, 64.9/79.8 cm^{-1} as ν_4, and 75.3/86.3 cm^{-1} as the ν_5 band.

Experiment and theory agree that a large frequency gap exists between ν_5 and the next fundamental, the phenol acceptor stretch σ_1; cf. Figure 5 and Table 4. The next bands, which are hard to explain by overtone or combination bands with respect to their frequencies and intensities, are observed at 185.8, 198.1, and 208.1 cm^{-1}, in reasonable agreement with the frequencies calculated for the intermolecular phenol donor stretch vibration σ_2 and the H_2O-H_2O stretch vibrations σ_3 and σ_4. Alterna-

Intermolecular Vibrations of Phenol(H$_2$O)$_{2-5}$

J. Phys. Chem. A, Vol. 102, No. 24, 1998 **4477**

Figure 6. Dispersed fluorescence spectra of phenol(H$_2$O)$_3$-h obtained via excitation of (a) the electronic origin band 0_0^0, (b) 0_0^0 + 18.9 cm^{-1}, and (c) 0_0^0 + 24.0 cm^{-1}. Vibrational frequencies are given in cm^{-1}.

tively, the bands at 198.1 and 208.1 cm^{-1} may be rather intense combination bands, e.g., $\sigma_1+\nu_4$ and $\sigma_1+\nu_5$, respectively.

The SHB of phenol(D$_2$O)$_3$-d_1 in Figure 5c generally supports the assignment given above; cf. Table 4. Bürgi et al. observed a band at 8.0 cm^{-1} as the lowest frequency S$_1$ band of phenol-(D$_2$O)$_3$-d_1.[7] This band has no match in the phenol(H$_2$O)$_3$ spectrum, and the authors speculate about the existence of a second conformer or isomer. We did not observe this band in the R2PI or SHB spectrum and can rule out a second conformer in the investigated wavelength range by our hole-burning experiments. The two-color R2PI spectra in ref 7 show no bands above ≈55 cm^{-1} for the deuterated cluster and no bands above ≈65 cm^{-1} for phenol(H$_2$O)$_3$ except for a very weak transition at 187 cm^{-1}. The SHB spectra (and partially also the one-color R2PI spectra shown in Figure 5) exhibit the whole wealth of stretch vibrations above 100 cm^{-1}. The higher frequency intermolecular vibrations tend to undergo fast intramolecular S$_1$ vibrational relaxation in the larger clusters. Therefore these transitions are weak or absent in the two-color ionization spectra. Small S$_1$ lifetimes, however, do not deteriorate the SHB signals, but may even increase the persistence of the burned spectral hole. We could already show this effect for the H acceptor spectrum of the phenol dimer.[25] The one-color R2PI spectra in Figure 5 point to less sensitivity with respect to the S$_1$ lifetime if excitation and ionization photons stem from the same laser pulse. The very different intensities of the SHB and R2PI spectra can also be traced back to the large power of the hole-burning laser which overdoes the intensities of weak bands.

TABLE 4: Intermolecular Vibrational Frequencies of Phenol(H$_2$O)$_3$-h and Phenol(D$_2$O)$_3$-d_1 in the S$_0$ and S$_1$ State. For Assignment See Text (All Frequencies Are Given in cm^{-1}). The Experimental Frequencies Are Averages of Several Experimental Scans. The Reproducibility Is ±0.5 cm^{-1}

experimental frequencies			assign-ment	calculated harmonic S$_0$ frequencies[7]	
S$_1$		S$_0$			
ph(H$_2$O)$_3$-h	ph(D$_2$O)$_3$-d_1	ph(H$_2$O)$_3$-h		ph(H$_2$O)$_3$-h	ph(D$_2$O)$_3$-d_1
36 257.8	36 289.4		0_0^0		
9.6	11.5	16.9	ν_1	21.3	20.5
18.9	20.4	33.2	$2\nu_1$		
24.0	25.1	26.6	ν_2	29.6	28.7
27.9		50.0	$3\nu_1$		
32.5	36.5		$\nu_1+\nu_2$		
39.3		41.8	ν_3	45.7	41.0
42.0	46.2		$2\nu_1+\nu_2$		
48.8	50.0	53.8	$2\nu_2$		
		57.5	$\nu_1+\nu_3$		
57.9	54.5	66.9	ν_4	69.3	67.3
64.9		79.8	ν_5	74.6	71.0
75.3		86.3			
78.2					
		90.6			
		94.9			
		100.0			
89.7			$\nu_2+\nu_5$		
100.4					
104.2					
		107.0			
		112.0			
		130.0			
134.3	131.8	154.0	σ_1	153.2	148.4
145.2	143.3		$\sigma_1+\nu_1$		
153.3			$\sigma_1+2\nu_1$		
158.3	157.6		$\sigma_1+\nu_2$		
	169.2		$\sigma_1+\nu_1+\nu_2$		
180.8			$\sigma_1+2\nu_2$		
185.8	179.4	187.5	σ_2	190.7	183.2
195.2		204.3	$\sigma_2+\nu_1$		
198.1	190.2	208.4	σ_3	217.1	205.2
		214.0	$\sigma_2+\nu_2$		
		220.6	$\sigma_2+2\nu_1$		
		229.0	$\sigma_2+\nu_3$		
201.0			$\sigma_1+3\nu_2$		
	198.2				
208.1	201.4		σ_4	237.6	224.7

4.3. R2PI, SHB, and DF Spectra of Phenol(H$_2$O)$_4$. Our ab initio calculations (HF/6-31G(d,p)) presented in section 3 reveal a cyclic minimum energy structure for this cluster with a *Dudud* arrangement of the phenyl ring and the free hydrogen atoms. The RIDIR spectrum in ref 9 exhibits five low-frequency OH stretch vibrations, in agreement with a cyclic structure. The SHB spectrum of the low-frequency intermolecular vibrations built upon the electronic origin at 36 170.4 cm^{-1} is displayed in Figure 7. The assignment of the mutual ring motions and the intermolecular stretch vibrations is given in Table 5. The assignment is supported by the SHB spectrum of phenol(D$_2$O)$_4$-d_1, which is shown in Figure 7c.

Again the three mutual ring motions ν_1, ν_2, and ν_3 are optically active, indicating a slight change of the ring orientations upon S$_1$ excitation. No progression in the ν_1 vibration is visible, indicating a smaller change in the angle between both rings compared to phenol(H$_2$O)$_3$. Similar to phenol(H$_2$O)$_2$ and phenol(H$_2$O)$_3$, all intermolecular stretch vibrations are optically active. Again we have a considerable frequency gap between the highest frequency oxygen ring deformation vibration ν_7 at 82.4 cm^{-1} and the lowest frequency phenol acceptor stretch vibration σ_1 at 130.6 cm^{-1}, in agreement with theory; cf. Table 2. The vibrational pattern of the stretch modes looks similar as in phenol(H$_2$O)$_3$. The frequency gap between the intense
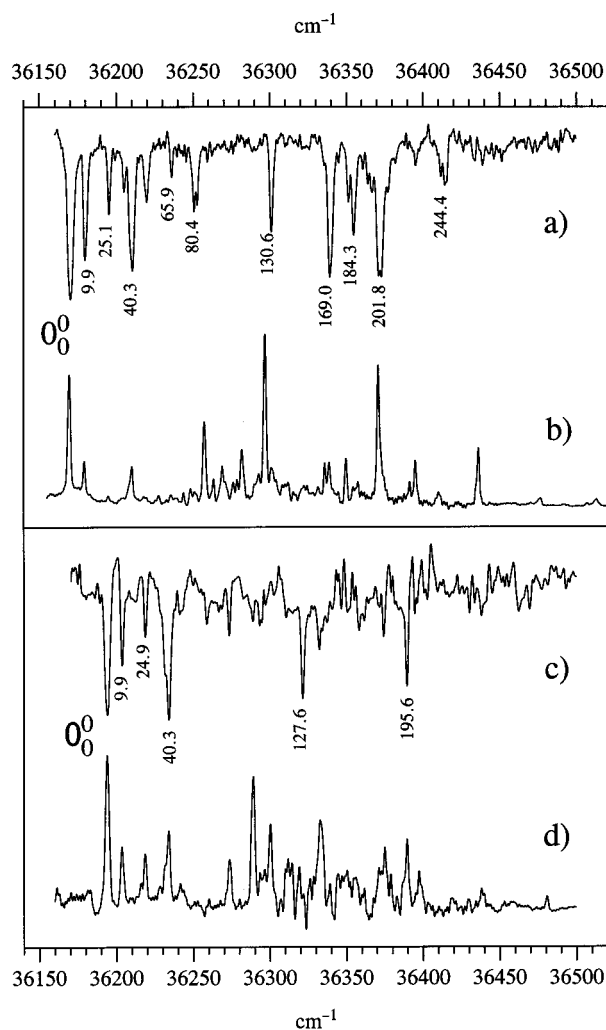
Figure 7. Hole burning and R2PI spectra of (a, b) phenol(H$_2$O)$_4$-*h* and (c, d) phenol(D$_2$O)$_4$-*d$_1$* obtained via analysis of the electronic origin bands at 36 170.4 and 36 194.0 cm^{-1}, respectively. Traces (a) and (c) show the SHB spectra. Vibrational frequencies are given in cm^{-1}.

low-frequency vibrations and the most intense intermolecular stretch vibrations is even more evident in the DF spectrum; cf. Figure 8a.

For some of the S$_1$ and S$_0$ bands an alternative assignment is possible. The 25.1/24.4 and 35.0/36.3 cm^{-1} vibrations may be interpreted as the first and second overtone of the ν_1 mode. In that case, ν_2 cannot be assigned.

4.4. R2PI, SHB, and DF Spectra of Phenol(H$_2$O)$_5$. R2PI measurements showed another intense band at 36 297.2 cm^{-1} when monitoring the phenol(H$_2$O)$_4$ mass channel (Figure 7b). Two-color ionization with the ionization laser fixed at 347.5 nm revealed no sign of this band on the phenol(H$_2$O)$_5$ mass channel.[2] Figure 9 shows that a number of low-frequency vibronic transitions are built upon this origin. From the SHB spectra it is apparent that the transitions in Figure 7 and Figure 9 do not share a common ground-state level. Hence they belong to different isomers or clusters of different size. The RIDIR spectrum in ref 9 shows more OH stretch bands than expected from a cluster with four water molecules. The ionization potentials and ion dissociation energies of larger phenol/water clusters are unknown, and they may fragment easily so that the RIDIR spectra could arise from a higher cluster.

From these considerations we repeated the two-color ionization experiment using the third harmonic of our Nd:YAG pump laser to ionize at 355 nm. The inset in Figure 9 shows that the
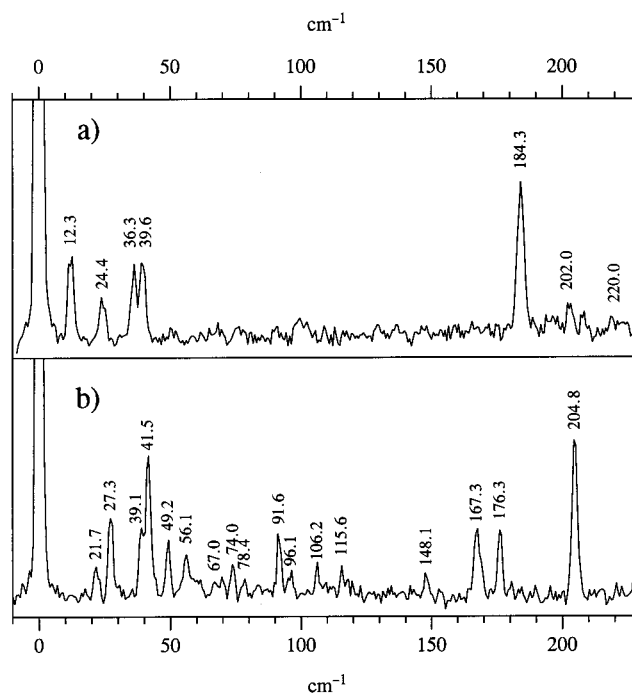
Figure 8. Dispersed fluorescence spectra of (a) phenol(H$_2$O)$_4$-*h* and (b) phenol(H$_2$O)$_5$-*h* obtained through the electronic origin bands at 36 170.4 and 36 297.2 cm^{-1}, respectively. Vibrational frequencies are given in cm^{-1}.
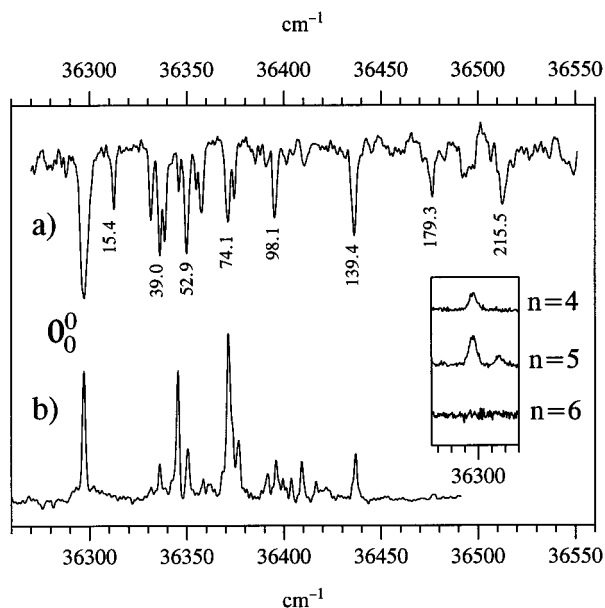
TABLE 5: Intermolecular Vibrational Frequencies of Phenol(H$_2$O)$_4$-*h* and Phenol(D$_2$O)$_4$-*d$_1$* in the S$_0$ and S$_1$ State. For Assignment See Text (All Frequencies Are Given in cm^{-1}). The Experimental Frequencies Are Averages of Several Experimental Scans. The Reproducibility Is ±0.5 cm^{-1}

experimental frequencies				calculated harmonic S$_0$ frequencies[7]	
S$_1$		S$_0$	assign-		
ph(H$_2$O)$_4$-*h*	ph(D$_2$O)$_4$-*d$_1$*	ph(H$_2$O)$_4$-*h*	ment	ph(H$_2$O)$_4$-*h*	ph(D$_2$O)$_4$-*d$_1$*
36 170.4	36 194.0		0^0_0		
9.9	9.9	12.3	ν_1	12.8	12.3
25.1	24.9	24.4	ν_2	25.8	24.7
35.0		36.3	$\nu_1 + \nu_2$		
40.3	40.3	39.6	ν_3	33.3	32.4
49.7	48.0		$2\nu_2$		
65.9	65.0		$\nu_2 + \nu_3$		
80.4	79.0	76.0	$2\nu_3$		
82.4			ν_7	79.0	75.2
130.6	127.6		σ_1	147.4	141.0
169.0	164.0		$\sigma_1 + \nu_3$		
180.1					
184.3	181.0	184.3	σ_2	187.5	185.1
201.8	195.6	202.0	σ_3	203.5	193.7
225.1					
241.6					
244.4		220.0	σ_4	241.6	228.9

band at 36 297.2 cm^{-1} indeed belong to the phenol(H$_2$O)$_5$ cluster. Comparison of the R2PI and the SHB spectrum in Figure 9 shows that only one isomer absorbs in the investigated spectral range.

In agreement with theory the RIDIR spectra in ref 9 show that with increasing cluster size the bound OH stretch vibrations shift to lower frequencies while the free OH stretch frequencies remain essentially constant. Therefore a frequency gap develops with an infrared absorption "window" in the range ≈3460−3700 cm^{-1} in the case of the cyclic phenol(H$_2$O)$_4$ cluster. There is no gap anymore in the RIDIR spectrum of the band at 36 297.0 cm^{-1}, as shown in refs 8 and 9. At least four vibrations are observed in the window region. Ab initio calculations on

Intermolecular Vibrations of Phenol(H$_2$O)$_{2-5}$

J. Phys. Chem. A, Vol. 102, No. 24, 1998 **4479**

Figure 9. Hole burning and R2PI spectra of phenol(H$_2$O)$_5$-h obtained by analyzing the electronic origin band at 36 297.2 cm^{-1}. Vibrational frequencies are given in cm^{-1}. The inset shows the two-color ionization spectra of the electronic origin band (36 297.2 + 28 169 cm^{-1}); see text.

TABLE 6: Intermolecular Vibrational Frequencies of Phenol(H$_2$O)$_5$-h in the S$_0$ and S$_1$ State. For Assignment See Text (All Frequencies Are Given in cm^{-1}). The Slash Indicates the Book/Cage Assignment). The Experimental Frequencies Are Averages of Several Experimental Scans. The Reproducibility Is ±0.5 cm^{-1}

experimental frequencies ph(H$_2$O)$_5$-h		assign- ment	calculated harmonic S$_0$ frequencies[7] ph(H$_2$O)$_5$-h	
S$_1$	S$_0$		book(1)	cage(1)
36 297.2		0_0^0		
15.4	21.7	ν_1	13.9	10.1
34.4	27.3	ν_2	27.8	28.8
39.0	39.1	ν_4/ν_3	38.9	32.7
41.5	41.5	ν_3/ν_4	47.3	50.0
48.8				
52.9				
57.9				
60.3				
74.1				
77.1				
	74.0			
	91.6			
98.1				
113.5				
139.4	148.1	σ_1	143.0	146.3
179.3	167.3	σ_2	167.0	155.5
195.9	176.3	σ_3	175.6	183.5
215.5	204.8	σ_5/σ_6	206.5	207.1

pure water clusters show that complexes with water molecules acting as double donors absorb in the frequency range between the free and bound OH stretch absorption. There are several possible structures that look cage-, prism-, book-, and boat-like for (H$_2$O)$_6$ and similar for phenol(H$_2$O)$_5$, as discussed in section 3. Four vibrations in the window region point to a structure with *two* double-donor water molecules, each with a symmetric and antisymmetric OH stretch vibration in the window region.[10,14] This result favors somewhat the cage structures.

Table 6 shows a comparison between the experimental S$_0$ and S$_1$ intermolecular vibrational frequencies and the calculated harmonic frequencies for the two most stable double-donor

structures of phenol(H$_2$O)$_5$. Again we find optical activity of the three low-frequency mutual ring motions and good FC factors for some of the intermolecular stretch vibrations. The assignment of the oxygen ring (or cage) deformation vibrations remains quite tentative. The weak band at 195.9 cm^{-1} may as well be ascribed to combination bands, e.g.,$\sigma_2+\nu_1$ (194 cm^{-1}).

The most remarkable feature is the absence of an intensity gap in the DF spectrum of phenol(H$_2$O)$_5$ (cf. Figure 8b). There are no intense bands from ≈100 to 185 cm^{-1} for the cyclic phenol(H$_2$O)$_3$ and from ≈40 to 180 cm^{-1} for the cyclic phenol-(H$_2$O)$_4$ clusters. The dense S$_0$ spectrum of phenol(H$_2$O)$_5$ especially in the range of the intermolecular stretch vibrations and the comparably high frequency of the intense phenol donor–water acceptor stretch vibration (204.8 cm^{-1} in phenol(H$_2$O)$_5$ compared to 187.1/184.3 cm^{-1} in phenol(H$_2$O)$_{3/4}$) seem to be typical for double proton donor compared to single donor structures. The relatively weak double-donor hydrogen bridges add further low-frequency stretch vibrations to the spectrum; cf. Figure 8a,b. The experimental findings exclude a cyclic (single donor) structure for phenol(H$_2$O)$_5$ but do not allow a distinction between structures with one double donor (book) and two double donor (cage) water molecules; cf. Table 2.

Altogether the frequencies match a little bit better to the book form, which is more stable according to the calculations; cf. Table 1. Especially the rather high frequency of the ν_1 vibration compared to phenol(H$_2$O)$_{3/4}$ is in better agreement with the book form than with the cage form. This may result from the additional stabilizing π–hydrogen interaction, which leads to a higher force constant for the butterfly vibration. However, there are other book and cage isomers whose ν_1 frequencies match the experimental values better. Phenyl substitution in position 2 of the book and cage structures in Figure 3 lead to "double-acceptor" phenol, with considerably higher force constants for the butterfly vibration compared to the single proton acceptor phenol and higher vibrational frequencies ($\nu_1^{\text{cage(2)}} = 21$ cm^{-1}, $\nu_1^{\text{book(2)}} = 20$ cm^{-1} compared to 21.7 cm^{-1} from the experiment).

The differences between the intermolecular vibrational frequencies of the different double-donor structures of phenol-(H$_2$O)$_5$ are too small to allow for an unambiguous structural assignment of this cluster. It can be stated that the spectra in Figure 9 and Figure 8b stem from a noncyclic, more compact hydrogen-bonded network of phenol with five water molecules with at least one but probably two water molecules acting as double proton donors.

5. Conclusions and Outlook

We have shown in this paper that spectral hole burning and dispersed fluorescence are valuable tools to provide a nearly complete picture of the intermolecular vibrations in small clusters. Contrary to R2PI, SHB proves to be sensitive to the higher frequency intermolecular vibrations which tend to fast relaxation in molecular aggregates with high vibrational state densities.

The DF data can be compared directly with the calculated intermolecular frequencies for the electronic S$_0$ ground state and turn out to be sensitive for discrimination of single proton donor and double donor structures. Our assignment of the S$_0$ intermolecular vibrations is based on a harmonic model that is probably a qualitatively valid description for the mutual ring motions ν_1, ν_2, and ν_3 (cf. the overtone and combination bands in Tables 4, 5) and the intermolecular stretch vibrations and their overtones.[25,26] We expect considerable anharmonicity at least for the hydrogen torsion vibrations that could not be assigned in this paper.

4480 *J. Phys. Chem. A, Vol. 102, No. 24, 1998*

Jacoby et al.

In ref 27 we showed that the torsional tunneling of the water moiety in phenol$(H_2O)_1$ splits all vibronic levels in the S_1 state. Especially the intermolecular in-plane wag vibration β_2 exhibits a large splitting, which points to a strong coupling with the water torsion τ and a substantial lowering of the effective torsional barrier after β_2 excitation. The splitting of the stretch vibration, however, is small and very similar to the splitting of the electronic origin.[27,28] We did not find any hints on torsional splittings in phenol$(H_2O)_{2-5}$.

DF spectroscopy of single vibronic level fluorescence allows for an assignment of S_1 and S_0 vibrations based on intensity considerations. The underlying molecular motions in the S_1 state, however, where the electron density and phenol−OH bonding change significantly,[21] may not correspond to those in the ground state due to the Duschinsky effect.

UV double-resonance spectroscopy with population analysis via two-color ionization near the ionization threshold of the respective cluster seems to be the ideal tool for a spectroscopical access to examine larger clusters. The discrimination of possible isomers and a nearly complete picture of the most important intermolecular vibrations may be within reach.

References and Notes

(1) Lipert, R. J.; Colson, S. D. *J. Phys. Chem.* **1989**, *93*, 3894.

(2) Stanley, R. J.; Castleman, A. W. *J. Chem. Phys.* **1991**, *94*, 7744.

(3) Lipert, R. J.; Colson, S. D. *Chem. Phys. Lett.* **1989**, *161*, 303.

(4) Leutwyler, S.; Bürgi, T.; Schütz, M.; Taylor, A. *Faraday Discuss.* **1994**, *97*, 285.

(5) Gerhards, M.; Kleinermanns, K. *J. Chem. Phys.* **1995**, *103*, 7392.

(6) Schmitt, M.; Müller, H.; Kleinermanns, K. *Chem. Phys. Lett.* **1994**, *218*, 246.

(7) Bürgi, T.; Schütz, M.; Leutwyler, S. *J. Chem. Phys.* **1995**, *103*, 6350.

(8) Mikami, N. *Bull. Chem. Soc. Jpn.* **1995**, *68*, 683.

(9) Watanabe, T.; Ebata, T.; Tanabe, S.; Mikami, N. *J. Chem. Phys.* **1996**, *105*, 408.

(10) Watanabe, T.; Iwata, S. *J. Chem. Phys.* **1996**, *105*, 420.

(11) Bergmann, Messgeräte Entwicklung (BME), Ohlstadt.

(12) Schütz, M.; Bürgi, T.; Leutwyler, S.; Fischer, T. *J. Chem. Phys.* **1993**, *98*, 3763.

(13) Frisch, M. J.; Trucks, G. W.; Schlegel, H. B.; Gill, P. M. W.; Johnson, B. G.; Robb, M. A.; Cheeseman, J. R.; Keith, T.; Petersson, G. A.; Montgomery, J. A.; Raghavachari, K.; Al-Laham, M. A.; Zakrzewski, V. G.; Ortiz, J. V.; Foresman, J. B.; Peng, C. Y.; Ayala, P. Y.; Chen, W.; Wong, M. W.; Andres, J. L.; Replogle, E. S.; Gomperts, R.; Martin, R. L.; Fox, D. J.; Binkley, J. S.; Defrees, D. J.; Baker, J.; Stewart, J. P.; Head-Gordon, M.; Gonzalez, C.; Pople, J. A. *Gaussian 94*; Gaussian, Inc.: Pittsburgh, PA, 1995.

(14) Roth, W.; Gerhards, M.; Schumm, S.; Kleinermanns, K. In preparation.

(15) http://www-public.rz.uni-duesseldorf.de/~pc1/gauss/phxw.html.

(16) For detailed information about the programs GAUSSVIEW (http://www.gaussian.com), MOLDEN (http://caos.cam.kun.nl/), or XMOL (http://www.msc.edu/msc/docs/xmol/XMol/html), see our homepage.[15]

(17) Gregory, J. K.; Clary, D. C. *J. Phys. Chem.* **1996**, *100*, 18014.

(18) Gregory, J. K.; Clary, D. C. *J. Phys. Chem. A* **1997**, *101*, 6813.

(19) Liu, K.; Brown, M. G.; Carter, C.; Saykally, R. J.; Gregory, J. K.; Clary, D. C. *Nature* **1996**, *381*, 501.

(20) Pohl, M.; Schmitt, M.; Kleinermanns, K. *J. Chem. Phys.* **1991**, *94*, 1717.

(21) Berden, G.; Meerts, W. L.; Schmitt, M.; Kleinermanns, K. *J. Chem. Phys.* **1996**, *104*, 972.

(22) Connell, L. L.; Ohline, S. M.; Joireman, P. W.; Corcoran, T. C.; Felker, P. M. *J. Chem. Phys.* **1991**, *94*, 4668.

(23) Knochenmuss, R.; Leutwyler, S. *J. Chem. Phys.* **1989**, *91*, 1268.

(24) Schmitt, M. Doctoral Thesis, Heidelberg, 1992.

(25) Schmitt, M.; Henrichs, U.; Müller, H.; Kleinermanns, K. *J. Chem. Phys.* **1995**, *103*, 9918.

(26) Henrichs, U. Doctoral Thesis, Düsseldorf, 1996.

(27) Schmitt, M.; Jacoby, Ch.; Kleinermanns, K. *J. Chem. Phys.* **1998**, *108*, 4486.

(28) Vogel, H.-P.; Helm, R.; Neusser, H. J. *J. Chem. Phys.* **1998**, *108*, 4496.